

Effects of Ca(Y)-Si modifier on interface morphology and solute segregation during directional solidification of an austenite medium Mn steel

Gaofei Liang, Zhenming Xu, and Jianguo Li

School of Environmental Science and Engineering, Shanghai Jiaotong University, Shanghai 200240, China

(Received 2004-08-22)

Abstract: The austenite medium Mn steel modified with controlled additions of Ca, Y, Si were directionally solidified using the vertical Bridgman method to study the effects of Ca(Y)-Si modifier on the solid-liquid (S-L) interface morphology and solute segregation. The interface morphology and the C and Mn segregation of the steel directionally solidified at 6.9 $\mu\text{m/s}$ were investigated with an image analysis and a scanning electron microscope equipped with energy dispersive X-ray analysis. The 0.5wt% Ca-Si modified steel is solidified with a planar S-L interface. The interface of the 1.0wt% Ca-Si modified steel is similar to that of the 0.5wt% Ca-Si modified steel, but with larger nodes. The 1.5wt% Ca-Si modified steel displays a cellular growth pattern. The S-L interface morphology of the 0.5wt% Ca-Si+1.0wt% Y-Si modified Mn steel appears as dendritic interface, and primary austenite dendrites reveal developed lateral branching at the quenched liquid. In the meantime, the independent austenite colonies are formed ahead of the S-L interface. A mechanism involving constitutional supercooling explains the S-L interface evolution. It depends mainly on the difference in the contents of Ca, Y, and Si ahead of the S-L interface. The segregation of C and Mn ahead of the S-L interface enhanced by the modifiers is observed.

Key words: austenite Mn steel; modification; solid-liquid (S-L) interface morphology; solute segregation; directional solidification

[This work is financially supported by the National Natural Science Foundation of China (No.50001008 and No. 50271042).]

1 Introduction

Austenite medium Mn steel is still a popular wear resistant material. Its wear resistance increases with the increment of C content, while the toughness will decrease greatly because the network and/or needle-like carbides appear in the austenite matrix [1]. It has been reported that the diffusion-controlled precipitation of these carbides can be impeded, meanwhile granular $\gamma\text{-(Fe, Mn)}_3\text{C}$ eutectics appear in the as-cast austenite medium Mn steel modified with Si-containing agents [2-3]. It is therefore believed that the modifiers exert a great influence on the eutectic formation. Some experiments have been performed to investigate the effects of cooling rate and modifier amount on the microstructure selection of the austenite medium Mn steel and the scales of eutectics such as volume fraction and diameter [4]. The discussions on the effects of modifiers on the segregation of C and Mn during the solidification of austenite medium Mn steels have been given in reference [2]. However, characterizing the relationship between the modifier amount and segregation degree in the classical sand cast state is probably influenced by cooling

rate. In directional solidification, cooling rate and modifier amount can be independently controlled so that one may study the dependence of segregation on either the cooling rate at a constant modifier amount or the modifier amount at a constant cooling rate. Therefore, the directional solidification of the austenite medium Mn steel modified with controlled additions of Ca, Y, and Si has been carried out using the vertical Bridgman method. The results from these solidified alloys in this paper will illustrate the effects of Ca(Y)-Si modifier on the solid-liquid interface morphology and C and Mn segregation, in order to get a better understanding of the growth behavior and the modification mechanism for the austenite medium Mn steel.

2 Experimental procedure

The master samples were prepared by melting weighed quantities of pig iron, steel scraps, Fe-Mn alloy (wt%) (Fe-80Mn-1.0Si-1.2C), Al-Si alloy (Al-1.0Si-0.01Fe), Ca-Si agent (Fe-28Ca-65Si-2.4Al-0.8C), and Y-Si agent (Fe-12Y-44Si-2Mn). After the allowing time for melt homogenization, the molten

alloy was poured into the prepared bar molds. The nominal composition of the cast steels is listed in ta-

ble 1.

Table 1 Chemical composition of master samples for directional solidification

wt%

Sample	Quantity of modifier	Nominal composition								
		C	Mn	Si	Al	Ca	Y	S	O	Fe
No.1	Ca-Si/0.5	1.25	6.60	0.67	1.00	0.14	—	0.02	0.02	Bal.
No.2	Ca-Si/1.0	1.25	6.60	1.06	1.06	0.30	—	0.02	0.02	Bal.
No.3	Ca-Si/1.5	1.25	6.60	1.75	1.08	0.45	—	0.02	0.02	Bal.
No.3	Ca-Si/0.5+Y-Si/1.0	1.25	6.60	1.63	1.06	0.14	0.10	0.02	0.02	Bal.

Directional solidification was performed using a high temperature gradient Bridgman-type unit in the protective argon atmosphere. Detailed descriptions of the unit were given elsewhere [5]. The specimens were directionally solidified at a constant pulling speed of $6.9 \mu\text{m/s}$ with a constant temperature gradient of about 800 K/cm . The assumption was made that the growth rate is equal to the pulling speed according to reference [6]. They were quenched rapidly into alloys reservoir after 30 mm steady growth. The samples were ground, polished, and etched in a solution of 4 mL HNO_3 and 96 mL $\text{C}_2\text{H}_5\text{OH}$.

The microstructure and solute distribution in the quenched liquid ahead of the solid-liquid (S-L) interface were examined by using an image analysis (IA) and a scanning electron microscope (SEM) equipped with energy dispersive X-ray analysis (EDXA). The

average value of line scan data was calculated by using the Microsoft Excel software.

3 Results and discussion

3.1 S-L interface morphology and solidified microstructure

Figures 1(a)-(d) show the optical micrographs of the S-L interfaces in steels No.1-No.4 directionally solidified at $6.9 \mu\text{m/s}$. Steel No.1 is solidified with a planar S-L interface. The interface of steel No.2 is similar to that of steel No.1, but with larger nodes. Steel No.3 displays a cellular growth pattern. The dendritic interface appears, and the developed lateral branching of primary austenite dendrites into the quenched liquid and independent austenite colonies (see figure 1(d), marked by a solid arrow) ahead of the interface are observed in steel No.4.

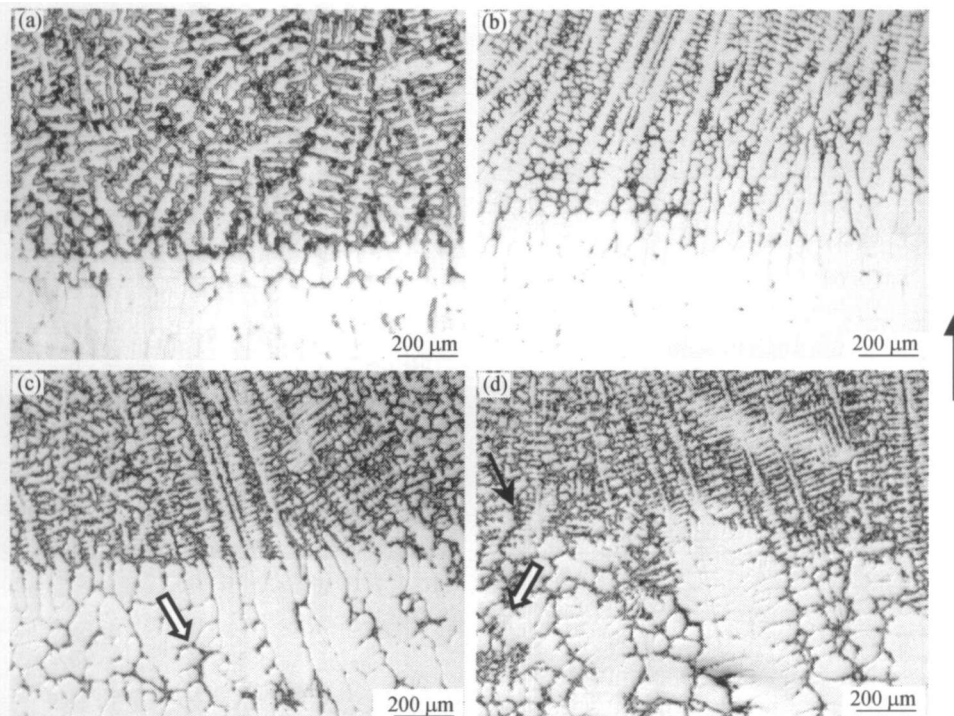


Figure 1 Solid-liquid (S-L) interfaces of directionally solidified steels at $6.9 \mu\text{m/s}$: (a) No.1; (b) No.2; (c) No.3; (d) No.4 (the arrow indicates the growth direction).

Figure 2 shows the microstructure of steel No.2 directionally solidified at $6.9 \mu\text{m/s}$. The solid at a distance of $550 \mu\text{m}$ to the S-L interface contains single austenite, but without any other phases. The solid near

the S-L interface in steel No.1 is the same as that in steel No.2 (see figure 1(a)). Otherwise, the solid near the S-L interfaces in steels No.3 and No.4 contains austenite in which a few C(Mn)-richer phases

distribute among the dendrites (see figures 1(c) and (d), marked by a hollow arrow).

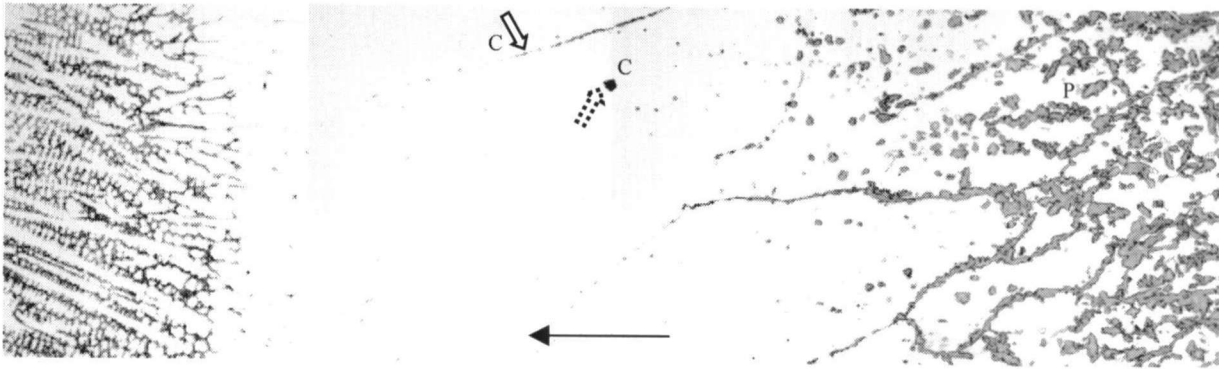


Figure 2 Microstructure morphology for steel No.2 directionally solidified at 6.9 μm/s, where carbide is marked by C, and pearlite by P (the arrow indicates the growth direction).

3.2 Solute segregation ahead of the S-L interface

Figures 3(a) and (b) show the SEM micrographs of the S-L interfaces and the corresponding Si and Ca line scan images of the directionally solidified steels No.1 and No.2, respectively. It is seen that the quenched liquid ahead of the S-L interface in steel No.2 contains a higher level of Si and Ca than steel No.1. It is consistent with the nominal composition (see table 1). Figure 3(c) presents the secondary

electron images with corresponding Y and Si line scan maps of the S-L interface in steel No.4. The EDXA point analysis shows that the composition of the area where Y content is the lowest along the scan line (see figure 3(c), marked by A) is as follows (wt%): C, 2.08; Si, 41.51; Mn, 7.27; Y, 0.74; Ca, 0.10, Fe, balance; as shown in figure 3(d). Clearly Y content ahead of the S-L interface is much larger than its nominal composition in the matrix (see table 1).

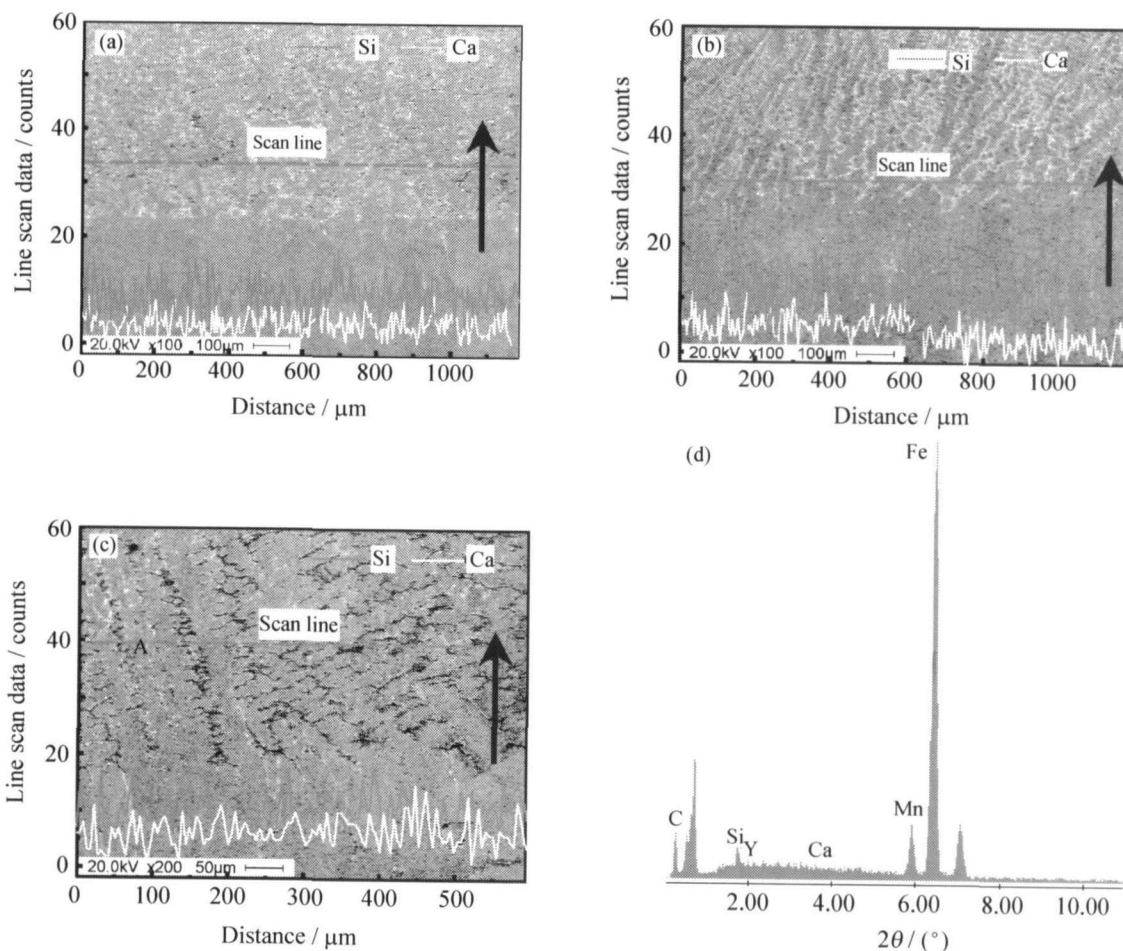


Figure 3 Quenched S-L interfaces and corresponding Y, Si and Ca line scan data of the steels: (a) No.1; (b) No.2; (c) No.4; (d) EDXA analysis result on the area marked by A in (c). The distance between the scan line and S-L interface is fixed at about 100 μm. The arrows indicate the growth direction. The scan rate is fixed at about 950-1000 CPS.

Figures 4(a)-(c) show the SEM micrographs of the S-L interfaces and the corresponding C and Mn line

scan images of the directionally solidified steels No.1, No.2, and No.4, respectively. The average line scan data of C and Mn are calculated by using the Microsoft Excel software. The results are presented in

figure 5. It can be seen that the quenched liquid ahead of the S-L interface in steel No.2 contains a higher level of C and Mn than steels No.1 and No.4.

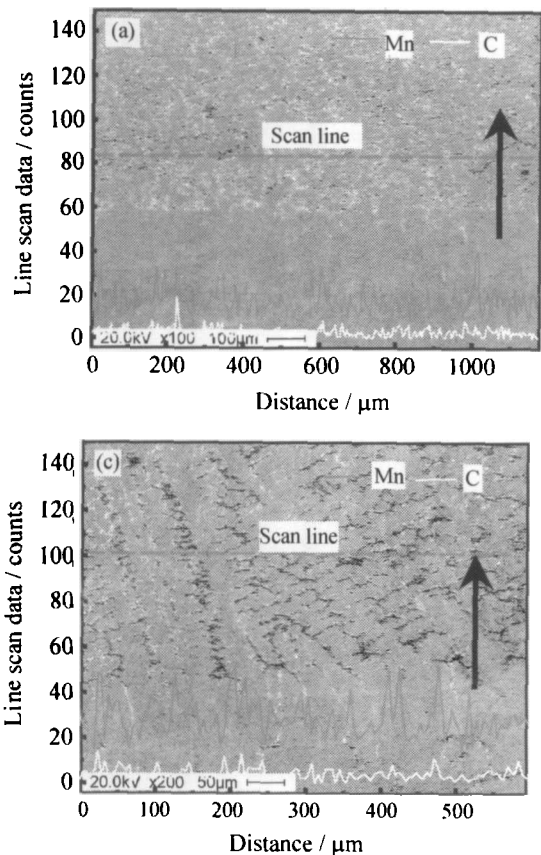


Figure 4 Quenched S-L interfaces and corresponding C and Mn line scan data of the steels: (a) No.1; (b) No.2; (c) No.4. The distance between the scan line and S-L interface is fixed at about 100 μm. The arrows indicate the growth direction. The scan rate is fixed at about 950-1000 CPS.

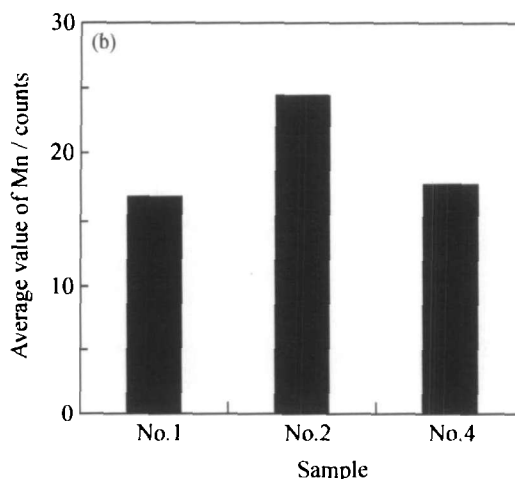
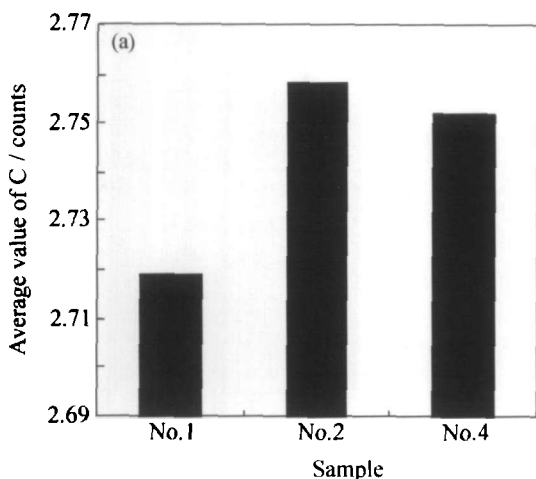


Figure 5 Average values of the line scan data of the steels corresponding to figure 4: (a) C; (b) Mn.

An effect of constitutional supercooling is the breakdown of a planar interface into cellular and dendritic growth. The instability of the interface arising with increasing the Ca-Si modifier amount is probably the result of constitutional supercooling. The equilibrium partition coefficients of Si and Ca are 0.83, and 0.56, respectively [7]. The constitutional supercooling develops when a higher level of Si, and Ca segregates ahead of the S-L interface. It leads to the change of the S-L interface shape from planar to cellular growth

parttern (see figures 1(a)-(c)). The equilibrium partition coefficient of Y is approximately equal to zero [8]. This indicates that Y segregates severely (see figures 3(c) and (d)). The fact that the S-L interface of steel No.4 is most instable may result from it according to the classical theory of constitutional supercooling.

In describing the segregation degree of solute *i* ahead of the planar growth front when the growth rate is very low, it is convenient to define the segregation ratio, SR_i [9]:

$$SR_i = C_{i,L}/C_{i,S} \quad (1)$$

where $C_{i,L}$, $C_{i,S}$ are the contents of solute i in the liquid and solid, respectively. The larger SR indicates solute i segregates severely if the equilibrium partition coefficient of solute i (k_i) is less than 1. Both k_C and k_{Mn} values are less than 1. Therefore, for element C (or Mn), the higher the $C_{C,L}$ (or $C_{Mn,L}$), the larger the SR_C (or SR_{Mn}) according to equation (1), and the more severely the C (or Mn) segregates.

Steels No.1 and No.2 are solidified with a planar S-L interface, as a result, no eutectic is formed among the ausentic dendrites during solidification (see figures 1(a) and (b)). In addition, some carbides are formed during subsequent cooling to the eutectoid temperature. C and Mn partitioning occurs primarily at the boundary (see figure 2, marked by a hollow arrow), followed by the regions richer in C and Mn inside the grain (see figure 2, marked by a dot hollow arrow). Below the eutectoid temperature, the austenite may be unstable and transform to pearlite during cooling [10]. The redistribution of C and Mn in the solid near S-L interface has not met the thermodynamics conditions during subsequent quenched cooling after solidification. Therefore, the solid at a distance of 550 μm to the S-L interface in steel No.2 (or No.1) contains single austenite, but without any other phases (see figures 1(a) and (b), and figure 2). From this discussion, it is clear that equation (1) can be used to describe the segregation of C and Mn ahead of the S-L interface in steels No.1 and No.2. Figure 5 shows that the quenched liquid ahead of the interface in steel No.2 contains a higher level of C and Mn than steel No.1, indicating the segregation of C and Mn increases with increasing the Ca-Si modifier amount.

The solid near the S-L interfaces in steels No.3 and No.4 contains austenite in which a few C(Mn)-richer phases distribute among the dendrites (see figures 1(c) and (d), marked by a hollow arrow). Therefore, equation (1) is not used to discuss the segregation of C and Mn in steels No.3 and No.4 because it is impossible to confirm the $C_{i,S}$ value. The EDXA analysis shows that the composition of these phases corresponds to the eutectic. Moreover, the distance to the S-L interface is within 550 μm . It therefore seems most likely that these phases are formed after the remaining liquid among austenite dendrites being quenched. The richer C and Mn in the remaining liquid among primary austenite dendrites (see figures 1(c) and (d), marked by a hollow arrow) indicates that the C and Mn contents ahead of the S-L interface decrease.

Consequently, the quenched liquid ahead of the interface in steel No.4 contains a lower level of C and Mn than steel No.2.

4 Conclusions

(1) The 0.5wt% Ca-Si modified steel is solidified with a planar S-L interface. The interface of the 1.0wt% Ca-Si modified steel is similar to that of the 0.5wt% Ca-Si modified steel, but with larger nodes. The 1.5wt% Ca-Si modified steel displays a cellular growth parttern. The S-L interface morphology of the 0.5wt% Ca-Si+1.0wt% Y-Si modified Mn steel appears as dendritic interface, and primary austenite dendrites reveal developed lateral branching at the quenched liquid. The independent austenite colonies are formed ahead of the S-L interface

(2) The modifiers enhance the segregation of C and Mn during the solidification of the austenite medium Mn steel.

References

- [1] G.F. Liang, Z.M. Xu, and J.G. Li, Effect of sliding velocity on the frictional behaviors of in situ granular eutectics reinforced austenite steel matrix composites, *Acta Metall. Sin.* (in Chinese), 39 (2003), No.5, p.550.
- [2] G.F. Liang, Z.M. Xu, Q.H. Jiang, and J.G. Li, Effect of Ca-Si modifier on the solidification and microstructure of austenite medium Mn steel, *J. Mater. Sci. Lett.*, 22(2003), p.549.
- [3] Z.M. Xu, T.X. Li, and J.G. Li, Microstructure and properties of austenite-bainite steel matrix wear resistant composite reinforced by granular eutectics, *J. Mater. Sci.*, 36(2001), p.4543.
- [4] G.F. Liang, Z.M. Xu,, and J. Li, Effects of growth rate and amount of Ca-Si modifier on the microstructure scales of granular eutectics in an austenite medium Mn steel, *Mater. Sci. Eng. A.*, A369(2004), p.157.
- [5] C.C. Ji, W.Z. Ma, J.G. Li, and Y.H. Zhou, Technique of melting and casting of (TbDy)Fe₂ matrix alloy bars, *J. Alloy Compd.*, 327(2001), p.220.
- [6] M. Gunduz and Çadirli, Directional solidification of aluminium-copper alloys, *Mater. Sci. Eng.*, 327A(2002), p.167.
- [7] C. Bodsworth and H.B. Bell, *Physical Chemistry of Iron and Steel Manufacture*, Longmans, London, 1972.
- [8] Z.S. Yu, *RE in the Steel*, Metallurgical Industry Press, Beijing, 1982.
- [9] H.Q. Hu, *Metal Solidification* (in Chinese) [M], Metallurgical Industry Press, Beijing, 1982.
- [10] Q.H. Jiang, S.S. Wang, Z. Li, and Z.M. He, Effect of Si on the nodularization of carbide in as-cast manganese steel (in Chinese), *Chin. Sci. Bull.*, 16(1990), No.14, p.1167.